New Journal of Physics
An Institute of Physics and Deutsche Physikalische Gesellschaft Journal

Solar models and solar neutrino oscillations

John N Bahcall and Carlos Peña-Garay
Institute for Advanced Study, School of Natural Sciences, Princeton, NJ 08540, USA
E-mail: jnb@ias.edu and penya@ias.edu

New Journal of Physics **6** (2004) 63
Received 5 April 2004
Published 16 June 2004
Online at http://www.njp.org/
doi:10.1088/1367-2630/6/1/063

Abstract. We provide a summary of the current knowledge, theoretical and experimental, of solar neutrino fluxes and of the masses and mixing angles that characterize solar neutrino oscillations. We also summarize the principal reasons for performing new solar neutrino experiments and what we anticipate from future studies.

Contents

PII: S1367-2630(04)79061-8

1. Introduction

In this paper, we present a snapshot (taken on 1 March 2004) of the present status of solar neutrino theoretical research. We do not attempt to review the literature on this subject. For details of the extensive literature, the reader is referred to earlier, more comprehensive studies [1]–[19].

The related subject of solar neutrino experiments will be reviewed in this volume by McDonald [20]. We therefore do not discuss the experimental aspects of solar neutrino research in this paper, although we do emphasize the relation between theoretical ideas and predictions and solar neutrino measurements.

We begin in section 2 by summarizing our current theoretical knowledge of the solar neutrino fluxes. We then discuss in section 3 the numerical results regarding solar neutrino parameters and neutrino fluxes that have been inferred from solar neutrino and reactor experiments. Neutrinos are the first cosmological dark matter to be discovered. We describe in section 4 what solar and atmospheric neutrino experiments have taught us about the cosmological mass density of neutrinos. We summarize in section 5 the constraints on CPT in the neutrino sector that result from comparing solar neutrino experiments with reactor anti-neutrino experiments. Finally, in section 6 we discuss the reasons for undertaking future solar neutrino experiments and the scientific results that may be obtained from the proposed new experiments.

To establish the appropriate context for our discussion, we note that measurements of the speed of sound inside the Sun (via a technique called helioseismology, which is similar to terrestrial seismology) agree with solar model predictions to an rms accuracy of better than 0.1%. This excellent agreement between the measured and predicted sound speeds established, as early as 1996, that the solution of the 'solar neutrino problem' lay in new particle physics, not in new astrophysics [21].

2. Solar model fluxes

In this section, the discussion is based on the results reported in the recent paper [22]. Full numerical details of the solar models, BP04 and BP00 discussed below are available together with earlier solar models in this series, at the web site http://www.sns.ias.edu/∼jnb . In particular, the primordial hydrogen and helium mass fractions for the BP04 model discussed below are $X_0 = 0.7078$ and $Y_0 = 0.2734$, respectively, whereas the current surface abundances are $X_S = 0.7397$ and $Y_S = 0.2434$.

2.1. Fluxes from different solar models

Table 1, taken from [22], gives the calculated solar neutrino fluxes for a series of solar models calculated with different plausible assumptions about the input parameters. The range of fluxes shown for these models illustrates the systematic uncertainties in calculating solar neutrino fluxes. The second (third) column, labelled BP04 (BP04+), of table 1 presents the currently available best solar model calculations for the neutrino fluxes. The uncertainties are given in column 2.

Figure 1 presents the neutrino energy spectrum predicted by the BP04 solar model for the most important solar neutrino sources.

The model BP04+ was calculated with the use of new input data for the equation of state, nuclear physics and solar composition. The currently preferred model BP04, is similar to BP04+ except that BP04 does not include the most recent analyses of the solar surface composition [24],

Table 1. Predicted solar neutrino fluxes from solar models. The table presents the predicted fluxes, in units of 10^{10}(pp), 10^{9}(^{7}Be), 10^{8}(pep, ^{13}N, ^{15}O), 10^{6}(^{8}B, ^{17}F) and 10^{3}(hep) cm^{-2} s^{-1}. Columns 2–4 show BP04, BP04+ and the previous best model BP00 [4]. Columns 5–7 present the calculated fluxes for solar models that differ from BP00 by an improvement in one set of input data: nuclear fusion cross-sections (column 5), equation of state for the solar interior (column 6) and surface chemical composition for the Sun (column 7). Column 8 uses the same input data as for BP04 except for a recent report of the ^{14}N + p fusion cross-section. References to the improved input data are given in the text. The last two rows ignore neutrino oscillations and present the capture rates in SNU (1 SNU = 10^{-36} events (target atom)$^{-1}$ s^{-1}) for the chlorine and gallium solar neutrino experiments. Owing to oscillations, the measured rates are smaller: 2.6 ± 0.2 and 69 ± 4, respectively. The neutrino absorption cross-sections and their uncertainties are given in [23].

Source	BP04	BP04+	BP00	Nucl.	EOS	Comp.	^{14}N
pp	5.94 (1 ± 0.01)	5.99	5.95	5.94	5.95	6.00	5.98
pep	1.40 (1 ± 0.02)	1.42	1.40	1.40	1.40	1.42	1.42
hep	7.88 (1 ± 0.16)	8.04	9.24	7.88	9.23	9.44	7.93
^{7}Be	4.86 (1 ± 0.12)	4.65	4.77	4.84	4.79	4.56	4.86
^{8}B	5.82 (1 ± 0.23)	5.28	5.05	5.79	5.08	4.62	5.77
^{13}N	5.71 ($1^{+0.37}_{-0.35}$)	4.06	5.48	5.69	5.51	3.88	3.23
^{15}O	5.03 ($1^{+0.43}_{-0.39}$)	3.54	4.80	5.01	4.82	3.36	2.54
^{17}F	5.91 ($1^{+0.44}_{-0.44}$)	3.97	5.63	5.88	5.66	3.77	5.85
Cl	$8.5^{+1.8}_{-1.8}$	7.7	7.6	8.5	7.6	6.9	8.2
Ga	131^{+12}_{-10}	126	128	130	129	123	127

which conflict with helioseismological measurements. We prefer the model BP04 over the model BP04+ because the abundance of the lower heavy element used in calculating BP04+ causes the calculated depth of the solar convective zone to conflict with helioseismological measurements.

The error estimates, which are the same for the three models labelled BP04, BP04+ and ^{14}N in table 1 include the recent composition analyses.

Column 4 of table 1 presents the fluxes calculated using the preferred solar model, BP00 [4], which was posted on the archives in October 2000. The BP04 best-estimate neutrino fluxes and their uncertainties have not changed markedly from their BP00 values despite refinements in input parameters. The only exception is the CNO flux uncertainties, which have almost doubled due to the larger systematic uncertainty in the surface chemical composition as estimated in the present paper.

We describe improvements in the input data relative to BP00. Quantities that are not discussed here are the same as for BP00. Each class of improvement is represented by a separate column, columns 5–7, in table 1. The magnitude of the changes between the fluxes listed in the different columns of table 1 are one measure of the sensitivity of the calculated fluxes to the input data.

Column 5 contains the fluxes computed for a solar model that is identical with BP00 except that improved values for direct measurements of the ^{7}Be(p, γ)^{8}B cross-section [25, 26], and the calculated p–p and hep cross-sections [26]. The reactions that produce the ^{8}B and hep neutrinos

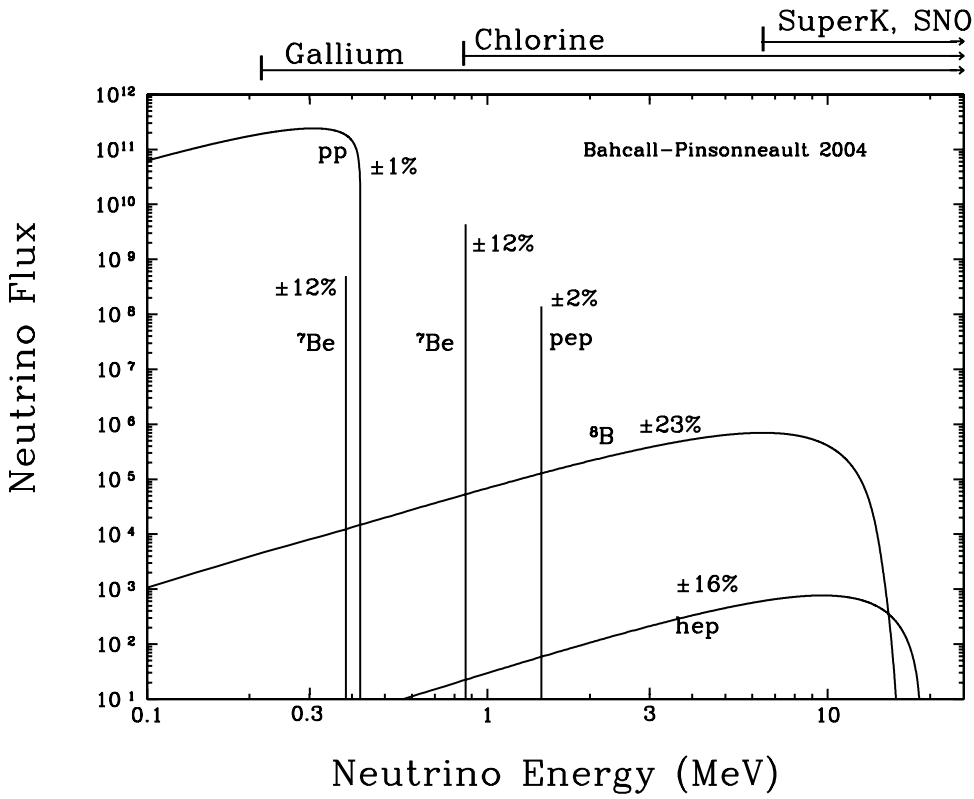

Figure 1. The predicted solar neutrino energy spectrum. The figure shows the energy spectrum of solar neutrinos predicted by the BP04 solar model [22]. For continuum sources, the neutrino fluxes are given in number of neutrinos $\mathrm{cm}^{-2}\,\mathrm{s}^{-1}\,\mathrm{MeV}^{-1}$ at the Earth's surface. For line sources, the units are number of neutrinos $\mathrm{cm}^{-2}\,\mathrm{s}^{-1}$. Total theoretical uncertainties taken from column 2 of table 1 are shown for each source. To avoid complication in the figure, we have omitted the difficult-to-detect CNO neutrino fluxes (see table 1).

are rare; changes in their production cross-sections affect only the ^{8}B and hep fluxes respectively. The 15% increase in the calculated ^{8}B neutrino flux, which is primarily due to a more accurate cross-section for $^7\mathrm{Be}(\mathrm{p},\gamma)^8\mathrm{B}$, is the only significant change in the best-estimate fluxes.

The fluxes in column 6 were calculated using a refined equation of state, which includes relativistic corrections and a more accurate treatment of molecules [27]. The equation of state improvements between 1996 and 2001, although significant in some regions of parameter space, change all the solar neutrino fluxes by $<1\%$. Solar neutrino calculations are insensitive to the present level of uncertainties in the equation of state.

The most important changes in the astronomical data from BP00 result from the new analyses of the surface chemical composition of the Sun. The input chemical composition affects the radiative opacity and hence the physical characteristics of the solar model, and to a lesser extent the nuclear reaction rates. New values for C, N, O, Ne and Ar have been derived [24] using three-dimensional rather than one-dimensional atmospheric models, including hydrodynamical effects, and paying particular attention to uncertainties in atomic data and observational spectra. New estimates of the abundance, together with the previous best estimates for other solar surface abundances [28], imply a ratio of heavy elements to hydrogen by mass of $Z/X = 0.0176$, much

Table 2. Principal sources of uncertainties in calculating solar neutrino fluxes. Columns 2–5 present the fractional uncertainties in the neutrino fluxes from laboratory measurements of the ^{3}He–^{3}He, ^{3}He–^{4}He, p–^{7}Be and p–^{14}N nuclear fusion reactions, respectively. The last four columns, 6–9, give the fractional uncertainties due to the calculated radiative opacity, the calculated rate of element diffusion, the measured solar luminosity and the measured heavy element to hydrogen ratio, respectively.

Source	3–3	3–4	1–7	1–14	Opacity	Diffusion	$L_\odot$	Z/X
pp	0.002	0.005	0.000	0.002	0.003	0.003	0.003	0.010
pep	0.003	0.007	0.000	0.002	0.005	0.004	0.003	0.020
hep	0.024	0.007	0.000	0.001	0.011	0.007	0.000	0.026
^{7}Be	0.023	0.080	0.000	0.000	0.028	0.018	0.014	0.080
^{8}B	0.021	0.075	0.038	0.001	0.052	0.040	0.028	0.200
^{13}N	0.001	0.004	0.000	0.118	0.033	0.051	0.021	0.332
^{15}O	0.001	0.004	0.000	0.143	0.041	0.055	0.024	0.375
^{17}F	0.001	0.004	0.000	0.001	0.043	0.057	0.026	0.391

less than the previous value of $Z/X = 0.0229$ [28]. Column 7 gives the fluxes calculated for this new composition mixture. The largest change in the neutrino flux for the p–p chain is the 9% decrease in the predicted ^{8}B neutrino flux. The N and O fluxes are decreased by much more, ∼35%, because they reflect directly the inferred C and O abundances.

The CNO nuclear reaction rates are less accurately determined than the rates for the more important (in the Sun) p–p reactions [29]. The rate for ^{14}N(p, γ)^{15}O is poorly known, but is important for calculating CNO neutrino fluxes. Extrapolating to the low energies relevant for solar fusion introduces a large uncertainty. Column 8 gives the neutrino fluxes calculated with an input data identical with BP04 except for the cross-section factor $S_0(^{14}\mathrm{N} + \mathrm{p}) = 1.77 \pm 0.2$ keV b that is about half the current best estimate; this value assumes a particular R-matrix fit to the experimental data [30]. The p–p cycle fluxes are changed by only ∼1%, but the ^{13}N and ^{15}O neutrino fluxes are reduced by 40–50% relative to the BP04 predictions. CNO nuclear reactions contribute 1.6% of the solar luminosity in the BP04 model and only 0.8% to the model with a reduced $S_0(^{14}\mathrm{N} + \mathrm{p})$.

2.2. Flux uncertainties

Table 2, also taken from [22], shows the individual contributions to the flux uncertainties. These uncertainties are useful in deciding how accurately we need to determine a given input parameter. Moreover, the theoretical flux uncertainties continue to play a significant role in some determinations of neutrino parameters from solar neutrino experiments (see e.g. [31]).

Columns 2–5 present the fractional uncertainties from the nuclear reactions whose measurement errors are most important for calculating neutrino fluxes. Unless stated otherwise, the uncertainties in the nuclear fusion cross-sections are taken from [29].

The measured rate of the ^{3}He–^{3}He reaction, which changed by a factor of 4 after the first solar model calculation of the solar neutrino flux [32], and the measured rate of the ^{7}Be + p reaction, which for most of this series has been the dominant uncertainty in predicting the ^{8}B neutrino flux, are now very well determined. If the current published systematic uncertainties

for the ^{3}He–^{3}He and ^{7}Be + p reactions are correct, then the uncertainties in these reactions no longer contribute in a crucial way to the calculated theoretical uncertainties (see columns 2 and 4 of table 2). This felicitous situation is the result of an enormous effort extending over four decades, and represents a great collective triumph for the nuclear physics community.

At present, the most important nuclear physics uncertainty in calculating solar neutrino fluxes is the rate of the ^{3}He–^{4}He reaction (see column 3 of table 2). The systematic uncertainty in the rate of ^{3}He(^{4}He, γ)^{7}Be reaction (see [29]) causes an 8% uncertainty in the prediction of both the ^{7}Be and the ^{8}B solar neutrino fluxes. It is scandalous that there has not been any progress in the last 15 years in measuring this rate more accurately.

For ^{14}N(p, γ)^{15}O, we have continued to use in table 2 the uncertainty given in [29], although the recent re-evaluation in [30] suggests that the uncertainty could be somewhat larger (see column 7 of table 1).

The uncertainties due to the calculated radiative opacity and element diffusion, as well as the measured solar luminosity (columns 6–8 of table 2), are all moderate, non-negligible but not dominant. For the ^{8}B and CNO neutrino fluxes, the uncertainties that are due to the radiative opacity, diffusion coefficient and solar luminosity are all in the range 2–6%.

The surface composition of the Sun is the most problematic and important source of uncertainties. Systematic errors dominate the effects of line blending, departures from local thermodynamic equilibrium and details of the model of the solar atmosphere. In the absence of detailed information to the contrary, it is assumed that the uncertainty in all important element abundances is approximately the same. The 3σ range of Z/X is defined as the spread over all modern determinations (see [3, 4, 32]), which implies that at present $\Delta(Z/X)/(Z/X) = 0.15$ (1σ), 2.5 times larger than the uncertainty adopted in discussing the predictions of the model BP00 [4]. The recent uncertainty quoted for oxygen, the most abundant heavy element in the Sun, is similar: 12% [24].

Heavier elements such as Fe affect the radiative opacity and hence the neutrino fluxes more strongly than the relatively lighter elements [4]. This is the reason for the difference between the fluxes calculated with BP04 and BP04+ (or between BP00 and Comp., see table 1) being less than that expected for the 26% decrease in Z/X. The abundances that have changed significantly since BP00 (C, N, O, Ne and Ar) are all for lighter species for which meteoritic data are not available.

The dominant uncertainty listed in table 2 for the ^{8}B and CNO neutrinos is the chemical composition, represented by Z/X (see column 9). The uncertainty ranges from 20% for the ^{8}B neutrino flux to ∼35% for the CNO neutrino fluxes. Since the publication of BP00, the best published estimate for Z/X decreased by 4.3σ (BP00 uncertainty) and the estimated uncertainty due to Z/X increased for ^{8}B(^{15}O) neutrinos by a factor of 2.5 (2.8). Over the past three decades, the changes have almost always been towards a smaller Z/X. The monotonicity is surprising since different sources of improvements have caused successive changes. Nevertheless, since the changes are monotonic, the uncertainty estimated from the historical record is large.

3. Experimentally determined solar neutrino parameters

3.1. Solar neutrino oscillations

Solar neutrino experiments have demonstrated that solar neutrinos undergo flavour conversion. Recently, the mechanism of conversion has been identified as neutrino oscillations, i.e. flavour

conversion induced by neutrino masses and mixing angles. The confirmation of the predicted neutrino oscillation deficit provided by the measurements from the Japanese reactor (anti)neutrino detector KamLAND [33] represents a triumph of several decades of research on solar neutrinos.

The Standard Model of particle physics has to be extended to include neutrino masses and mixing angles. Oscillation experiments are sensitive to mixing angles, defined by the non-trivial relation between flavour and mass neutrino fields. Oscillation experiments are not sensitive to absolute masses but to the differences of squared masses, i.e. global phases are not observable but relative phases are observable. A detailed discussion of the space of oscillation parameters can be found in [34].

Solar neutrino oscillations are characterized by just one function, the survival probability of electron neutrinos. Neutrino production, evolution and detection are the same for muon and tau neutrinos. For any solar neutrino observable, the conversion probability to μ neutrinos ($P_{e,\mu}$) or to τ neutrinos ($P_{e,\tau}$) appears only in the combination $P_{e,\mu} + P_{e,\tau}$.

The survival probability of electron neutrinos, P_{ee}, can be related to the survival probability, $P_{ee}^{2\nu}$, for effective two neutrino oscillations by the equation [35, 36]

$$P_{ee} = \cos^4\theta_{13} P_{ee}^{2\nu}(\Delta m^2, \theta_{12}; \cos^2\theta_{13} n_e) + \sin^4\theta_{13}, \tag{1}$$

where Δm^2 and θ_{1i} are differences in the squares of the masses $m_2^2 - m_1^2$ and the vacuum mixing angles, respectively. The effective two-neutrino problem is solved with a rescaled electron density, $\cos^2\theta_{13} n_e$. The effect of ΔM^2, the mass difference squared characteristic of atmospheric neutrinos $\left(m_3^2 - m_2^2 \cong m_3^2 - m_1^2\right)$, averages out in equation (1) for the energies and distances characteristic of solar neutrino propagation. Results from the CHOOZ reactor experiment [37, 38] places a strong upper bound on $\sin^2 2\theta_{13}$, implying that θ_{13} is close to 0 or $\pi/2$. Atmospheric and solar data select the first option ($\sin^2\theta_{13} < 0.052$ at 3σ [39]). Thus the main effect of a small allowed θ_{13} on the survival probability is the introduction of the factor $\cos^4\theta_{13}$ in equation (1).

The effective Hamiltonian for two-neutrino propagation in matter can be written conveniently in the familiar form [2, 3, 7, 35], [40]–[42]

$$H = \begin{pmatrix} \dfrac{\Delta m^2 \cos 2\theta_{12}}{4E} - \dfrac{\sqrt{2} G_F \cos^2\theta_{13} n_e}{2} & \dfrac{\Delta m^2 \sin 2\theta_{12}}{2E} \\ \dfrac{\Delta m^2 \sin 2\theta_{12}}{2E} & -\dfrac{\Delta m^2 \cos 2\theta_{12}}{4E} + \dfrac{\sqrt{2} G_F \cos^2\theta_{13} n_e}{2} \end{pmatrix}, \tag{2}$$

where E is the energy of the neutrino and G_F the Fermi coupling constant. The relative importance of the MSW matter term and the kinematic vacuum oscillation term in the Hamiltonian can be parametrized by the quantity, β, which represents the ratio of matter to vacuum effects. From equation (2), we see that the appropriate ratio is

$$\beta = \frac{2\sqrt{2} G_F \cos^2\theta_{13} n_e E_\nu}{\Delta m^2}. \tag{3}$$

The quantity β is the ratio of the oscillation length in matter to the oscillation length in vacuum. In convenient units, β can be written as

$$\beta = 0.22 \cos^2\theta_{13} \left[\frac{E_\nu}{1\,\text{MeV}}\right] \left[\frac{\mu_e \rho}{100\,\text{g cm}^{-3}}\right] \left[\frac{7 \times 10^{-5}\,\text{eV}^2}{\Delta m^2}\right], \tag{4}$$

where μ_e is the electron mean molecular weight ($\mu_e \approx 0.5(1+X)$, X is the mass fraction of hydrogen) and ρ is the total density. For the electron density at the centre of the standard solar model, $\beta = 0.22$ for $E = 1\,\mathrm{MeV}$, $\theta_{13} = 0$, and $\Delta m^2 = 7 \times 10^{-5}\,\mathrm{eV}^2$.

3.2. The vacuum–matter transition

For the large mixing angle (LMA) region ($\Delta m^2 > 10^{-5}\,\mathrm{eV}^2$), the daytime survival probability can be written to a good approximation in the following simple form [2, 3, 7, 36], [40]–[42]:

$$P_{ee} = \cos^4\theta_{13}(\tfrac{1}{2} + \tfrac{1}{2}\cos 2\theta_{12}^M \cos 2\theta_{12}), \tag{5}$$

where the mixing angle in matter is

$$\cos 2\theta_{12}^M = \frac{\cos 2\theta_{12} - \beta}{\sqrt{(\cos 2\theta_{12} - \beta)^2 + \sin^2 2\theta_{12}}}. \tag{6}$$

In equation (6), β is calculated at the location where the neutrino is produced. The evolution is adiabatic, i.e. the parameters in the Hamiltonian vary slowly enough to allow the created neutrino to follow the changing Hamiltonian eigenstate. Thus the survival probability depends on the initial and final density but not on the details of the density profile.

Figure 2 illustrates the energy dependence of the LMA survival probability, P_{ee}. If $\beta < \cos 2\theta_{12} \sim 0.4$ (for solar neutrino oscillations), the survival probability corresponds to vacuum averaged oscillations,

$$P_{ee} = \cos^4\theta_{13}(1 - \tfrac{1}{2}\sin^2 2\theta_{12}) \quad (\beta < \cos 2\theta_{12}, \text{vacuum}). \tag{7}$$

If $\beta > 1$, the survival probability corresponds to matter-dominated oscillations,

$$P_{ee} = \cos^4\theta_{13}\sin^2\theta_{12} \quad (\beta > 1, \text{MSW}). \tag{8}$$

The survival probability is approximately constant in either of the two limiting regimes, $\beta < \cos 2\theta_{12}$ and $\beta > 1$. The LMA solution exhibits a strong energy dependence only in the transition region between the limiting regimes. The quantity β is defined by equations (3) and (4).

At what neutrino energy does the transition take place between vacuum oscillations and matter oscillations? The answer to this question depends on which neutrino source is studied, since the fraction of the neutrino flux that is produced at a given radius (i.e. density and μ_e) differs from one neutrino source to another. The ^{8}B neutrinos are produced at much smaller radii (higher densities) than the p–p neutrinos; the ^{7}Be production profile is intermediate between the ^{8}Be and p–p neutrinos. According to the BP00 solar model, the critical energy at which $\beta = \cos 2\theta_{12}$ is, for $\tan^2\theta_{12} = 0.41$,

$$E(\text{crit}) \simeq \begin{cases} 1.8\,\mathrm{MeV}\ (^8\mathrm{B}); \\ 2.2\,\mathrm{MeV}\ (^7\mathrm{Be}); \\ 3.3\,\mathrm{MeV}\ (\text{p–p}). \end{cases} \tag{9}$$

The actual energies for p–p and ^{7}Be neutrinos are below the critical energy where they are produced. To a very good approximation, ^{8}B neutrinos are always in the MSW regime (equation (8)), while p–p and ^{7}Be neutrinos are in the vacuum-averaged regime (equation (7)).

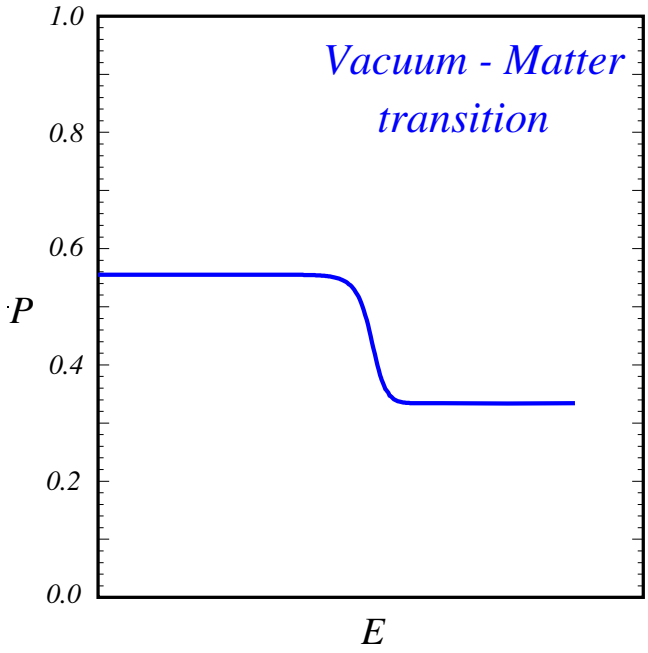

Figure 2. The electron neutrino survival probability, P_{ee}, as a function of neutrino energy for the (daytime) LMA oscillation solution. For small values of the parameter β defined in equations (3) and (4), the kinematic (vacuum) oscillation effects are dominant. For values of β greater than unity, the MSW (matter) oscillations are most important. For solar conditions, the transition between vacuum and matter oscillations occurs somewhere in the region of 2 MeV. A p–p (or pep) solar neutrino experiment would, together with the already-available results from ^{8}B solar neutrino experiments, test the predicted existence of the vacuum–matter transition (see discussion in section 6.3).

3.3. Experimentally determined solar neutrino parameters

All the results discussed in this section are taken from an analysis given in [9] for all currently available solar neutrino and reactor anti-neutrino experimental data. In this analysis, all solar neutrino fluxes are treated as free parameters subject only to the restriction that the fluxes satisfy the luminosity constraint. The evolution in the Sun and in the Earth of the neutrino wavefunctions is solved for numerically. The luminosity constraint imposes energy conservation provided that the Sun shines by nuclear fusion reactions among light elements [43]. Where numerical allowed intervals of a given parameter are reported, we marginalize over all other variables including θ_{13} and ΔM^2 atmospheric. At all points in oscillation parameter space, we use the value of all other variables that minimizes χ^2 for that set of parameters.

The best-fit values and the 1σ uncertainties for Δm^2 and $\tan^2\theta_{12}$ are

$$\Delta m^2 = (7.3^{+0.4}_{-0.6}) \times 10^{-5}\,\mathrm{eV}^2, \tag{10}$$

$$\tan^2\theta_{12} = 0.41 \pm 0.05. \tag{11}$$

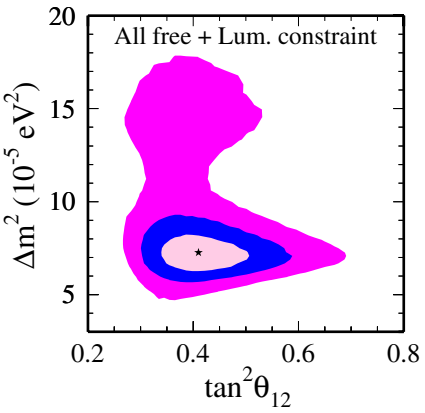

Figure 3. The allowed regions at 1σ, 2σ and 3σ. The allowed regions for neutrino oscillation parameters that are obtained in [9] by a global solution to all the available solar and reactor data. The neutrino fluxes are treated as free parameters subject only to the luminosity constraint.

Figure 3 shows the allowed regions for the oscillation parameters that are obtained at 1σ, 2σ and 3σ from the global solution (free neutrino fluxes subject only to the luminosity constraint) discussed in [9]. The allowed region at 3σ is 'fatter' than the corresponding region that is obtained when the solar neutrino fluxes are required to be consistent with the standard solar model predictions.

In principle, ν_e could oscillate into a state that is a linear combination of active (ν_a) and sterile (ν_s) neutrino states ($\nu_e \rightarrow \cos\eta\nu_a + \sin\eta\nu_s$). The allowed range 1σ for the active-sterile admixture is

$$\sin^2\eta \leqslant 0.10. \tag{12}$$

The result given in equation (12) implies that <6% of the ^{8}B flux is in the form of sterile neutrinos in the energy range observed by the Sudbury Solar Neutrino Observatory.

Comparing the measured neutrino fluxes with the theoretical predictions, we find that for BP04:

$$\phi(\mathrm{pp})_{\mathrm{measured}} = (1.02 \pm 0.02 \pm 0.01)\phi(\mathrm{pp})_{\mathrm{theory}}, \tag{13}$$

$$\phi(^8\mathrm{B})_{\mathrm{measured}} = (0.88 \pm 0.04 \pm 0.23)\phi(^8\mathrm{B})_{\mathrm{theory}}, \tag{14}$$

$$\phi(^7\mathrm{Be})_{\mathrm{measured}} = (0.91^{+0.24}_{-0.62} \pm 0.11)\phi(^7\mathrm{Be})_{\mathrm{theory}}. \tag{15}$$

In equations (13) and (15), the 1σ experimental uncertainties are given before the 1σ theoretical uncertainties.

The measured and theoretical values for the fluxes agree within their combined 1σ uncertainties. The measurement error of the ^{8}B neutrino flux is smaller than the uncertainty in the theoretical calculation, but the opposite is true for the p–p and ^{7}Be neutrino fluxes.

The CNO fluxes are poorly constrained by the available solar neutrino data (see [44]). BP04 predictions of the CNO-generated luminosity of the Sun (normalized to the measured

photon luminosity), $L_{\mathrm{CNO}} = 1.6 \pm 0.6\,\%$ are well inside the range allowed experimentally, $L_{\mathrm{CNO}} = 0.0^{+2.8}_{-0.0}\,\%$.

The results described above were obtained using the hypothesis that the Sun shines by nuclear fusion reactions among light elements. From neutrino measurements alone, one can measure the solar energy generation rate and then compare this neutrino luminosity with the photon luminosity being radiated from the solar surface. This comparison would test the fundamental idea that nuclear fusion reactions are responsible for the energy radiated by the Sun. Moreover, this same comparison would test a basic inference from the standard solar model, namely, that the Sun is in a quasi-steady state in which the energy currently radiated from the solar surface is balanced by the energy being produced by nuclear reactions in the solar interior at that moment. The ratio of the neutrino-inferred solar luminosity, $L_\odot$ (neutrino-inferred), to the accurately measured photon luminosity, $L_\odot$, is given by

$$\frac{L_\odot \text{ (neutrino-inferred)}}{L_\odot} = 1.4^{+0.2}_{-0.3}. \tag{16}$$

At present, the neutrino-inferred solar luminosity is still very uncertain. This result reflects once more the need for better determined low-energy neutrino fluxes.

What do we expect from larger data samples in currently running experiments? A global analysis using three years of data simulated for KamLAND shows that the uncertainty of Δm^2 (equation (10)) will be reduced by a factor of 2.5 [9]. SNO neutral current measurements (^{3}He counters) will be able to reduce the uncertainty of $\tan^2\theta_{12}$ by 20%. The neutrino fluxes summarized above are not affected, to the accuracy shown, by the additional simulated KamLAND data and improved SNO neutral current measurement.

4. Neutrinos as dark matter

Neutrinos are the first cosmological dark matter to be discovered. Solar and atmospheric neutrino experiments show that neutrinos have mass but these oscillation experiments only determine the differences between masses, not the absolute values. If we make the plausible but unproven assumption that the lowest neutrino mass, m_1, is much less than the square root of $\Delta m^2_{\mathrm{solar}}$, then we can conclude that the mass of cosmological neutrino background is dominated by the mass of the heaviest neutrino. This heaviest neutrino mass is then determined by $\Delta m^2_{\mathrm{atmospheric}}$. With this assumption the cosmological mass density in neutrinos is only [20, 39, 45]

$$\Omega_\nu = (0.0009 \pm 0.0001), \qquad m_1 \ll \sqrt{(\Delta m^2_{\mathrm{solar}})}. \tag{17}$$

Although the mass density given in equation (17) is small, it is of the same order of magnitude as the observed mass density in stars and gas.

The major uncertainty in determining the value of Ω_ν by neutrino experiments is the unknown value of the lowest neutrino mass. It is possible that neutrino masses are nearly degenerate and cluster around the highest mass scale allowed by direct β-decay experiments. If, for example, all neutrino masses are close to 1 eV, then $\Omega_\nu(1\,\mathrm{eV}) \sim 0.03$, which would be cosmologically significant.

More sensitive neutrino β-decay experiments and neutrinoless double β-decay experiments offer the best opportunities for determining the mass of the lowest mass neutrino and hence establishing the value of Ω_ν from purely laboratory measurements.

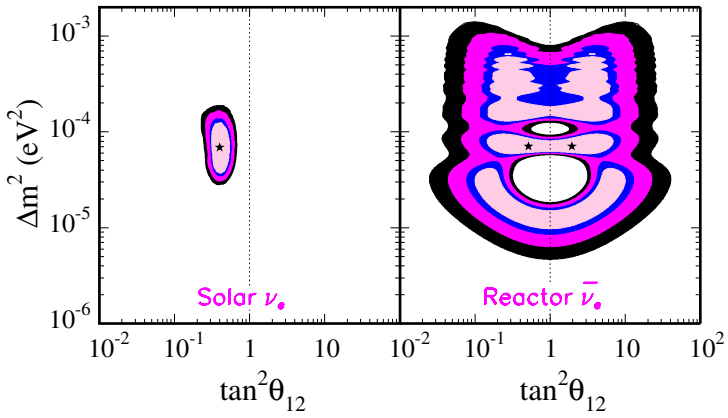

Figure 4. Neutrino and anti-neutrino oscillation constraints. The figure shows the 90, 95, 99%, and 3σ allowed regions for oscillation parameters that are obtained by a global solution to all the available solar data (left panel) or to all the available reactor data (right panel) [31]. The solar neutrino fluxes are treated as free parameters subject only to the luminosity constraint.

5. Test of CPT conservation with reactor and solar neutrino experiments

In this section, we compare the regions of allowed oscillation parameters for neutrinos and anti-neutrinos to constrain the violation of CPT in the neutrino sector [46]–[51]. Our discussion follows the pre-KamLAND analysis of [50], in which expected results from KamLAND were simulated.

Figure 4 shows, in the left-hand panel, the 90, 95, 99% and 3σ allowed regions for oscillation parameters that are obtained by a global solution to all the available solar data and, in the right-hand panel, to all the available reactor data [31]. The juxtaposition of purely solar and purely reactor data in the same figure allows a visual comparison of the constraints on neutrino and on anti-neutrino oscillation parameters. The allowed regions obtained by a global solution to all the available solar and reactor data are described in section 3.3 (see figure 3). The reactor data included in the analysis are from the CHOOZ [37] and KamLAND [33] experiments.

We characterize, following [50], the sensitivity of reactor and solar neutrino experiments to CPT violation by the quantity

$$\langle \Delta CPT \rangle = 2\frac{|\langle P_{\nu\nu}(E, L) - P_{\bar{\nu}\bar{\nu}}(E, L)\rangle|}{\langle P_{\nu\nu}(E, L) + P_{\bar{\nu}\bar{\nu}}(E, L)\rangle}. \tag{18}$$

Here both $P_{\nu\nu}(E, L)$ and $P_{\bar{\nu}\bar{\nu}}(E, L)$ are computed for the same experimental situation, but with different values for $(\Delta m^2_{\nu}, \theta_{\nu})$ and for $(\Delta m^2_{\bar{\nu}}, \theta_{\bar{\nu}})$ that are compatible with the allowed regions at a given CL shown in figure 4. The average in equation (18) is taken for a reactor distance, L, and over all neutrino and anti-neutrino energies, E. Then, $\langle \Delta CPT \rangle$ is the number of events observed in a reactor (anti-neutrino) experiment minus the number of events that would have been observed if neutrinos and anti-neutrinos had exactly the same oscillation parameters, divided by the average number of neutrino and anti-neutrino events.

The maximum value of $\langle \Delta CPT \rangle$ computed by comparing the survival probability in the 1σ (3σ) regions allowed by all solar neutrino data with the anti-neutrino survival probability in

the 1σ (3σ) regions allowed by all reactor data is given by

$$\langle \Delta CPT \rangle \leqslant 0.51\ (1.06) \quad \text{at } 1\sigma\ (3\sigma). \tag{19}$$

Matter effects, which simulate CPT violation, contribute <0.03 (0.08) to $\langle \Delta CPT \rangle$ for neutrino parameters in the 1σ (3σ) allowed regions.

This experimental upper limit on $\langle \Delta CPT \rangle$ can be used to test arbitrary future conjectures of CPT violation. Following [50], we consider an effective interaction which has been discussed by Coleman and Glashow [46, 47] and by Colladay and Kostelecky [48], that violates both Lorentz invariance and CPT invariance. The interaction is of the form

$$\mathcal{L}(\Delta CPT) = \bar{\nu}_{\mathrm{L}}^{\alpha} b_{\mu}^{\alpha\beta} \gamma_{\mu} \nu_{\mathrm{L}}^{\beta}, \tag{20}$$

where α, β are flavour indices, L indicates that the neutrinos are left-handed and b is a Hermitian matrix. We discuss the special case with rotational invariance in which b_0 and the mass-squared matrix are diagonalized by the same mixing angle. We also assume that there are only two interacting neutrinos (or anti-neutrinos) and follow the previous authors in defining η as the difference of the phases in the unitary matrices that diagonalize Δm^2 and the CPT odd quantity δb, which is the difference between the two eigenvalues of b_0.

When the relative phase is $\eta = 0$, the survival probabilities of neutrino and anti-neutrinos take on an especially simple form. For reactor anti-neutrinos, neutrinos oscillate in vacuum (matter effects are negligible in the range of parameters allowed by KamLAND data, see details in [31])

$$P_{\mathrm{ee}} = \cos^4\theta_{13}\left[1 - \sin^2 2\theta_{12}\sin^2\left(\frac{\Delta m^2 L}{4E} - \frac{\delta b L}{2}\right)\right]. \tag{21}$$

For solar neutrinos, sensitivity to δb in the oscillation phase is lost because of the fast oscillations due to the Δm^2 term. In the case of both solar and reactor neutrinos, the mixing in vacuum is unchanged. Equations (5) and (6) are valid with a modified ratio of matter to vacuum effects given by

$$\beta = \frac{2\sqrt{2} G_{\mathrm{F}} \cos^2\theta_{13} n_{\mathrm{e}} E_{\nu}}{\Delta m^2 + 2\delta b E}. \tag{22}$$

We have re-analysed solar and reactor neutrino data with the modified probabilities that contain an extra free parameter δb. We obtain the χ^2 distribution on δb by marginalizing over all other variables. The resulting bounds on violation of CPT invariance are

$$\delta b < 1.5(170) \times 10^{-21}\ \mathrm{GeV}, \qquad \eta = 0 \quad \text{at } 1\sigma\ (3\sigma). \tag{23}$$

The 3σ bound is much weaker than the 1σ bound. The reason is that the available KamLAND spectrum is compatible with no energy dependence at 2σ. Thus KamLAND cannot yet test at 3σ the specific CPT-violating model under discussion. The current bound at 3σ is due to CHOOZ reactor data with a baseline ~100 times shorter (CHOOZ imposes an upper bound on the allowed regions in the right panel of figure 4). If the expected energy dependence is confirmed in KamLAND, the 3σ limit can be significantly improved, to about $\delta b \sim 10^{-21}$ GeV (see [50]).

6. What can be learnt from new solar neutrino experiments?

We begin our discussion of new solar neutrino experiments by presenting in section 6.1 the four primary reasons for doing low-energy solar neutrino experiments. Next we discuss in sections 6.2, 6.3 and 6.4, respectively, what can be learnt from future ^{7}Be, p–p and pep solar neutrino experiments. Finally, we describe in section 6.5 what can be learnt from parasitic solar neutrino experiments that are carried out in connection with a next generation proton-decay experiment. The materials in sections 6.1–6.4 is based on [9].

6.1. Why low-energy solar neutrino experiments?

There are four primary reasons for performing low-energy solar neutrino experiments that measure the energy of individual neutrino-induced events.

First, new phenomena may be revealed at low energies (<3 MeV) that are not discernible at high energies (>5 MeV). According to the currently accepted LMA oscillation solution, the basic oscillation mechanism switches somewhere in the vicinity of 2 MeV (see equation (9) and figure 2) from the MSW matter-dominated oscillations that prevail at high energies to the vacuum oscillations that dominate at low energies. Does this transition from matter-induced to vacuum oscillations actually take place? If the transition does occur, is the ratio (β, see equations (3) and (4)) of the kinematic term in the Hamiltonian (i.e. $\Delta m^2/2E$) to the matter-induced term ($\sqrt{2}G_{\rm F}n_{\rm e}\cos^2\theta_{13}$) the only parameter that determines the physical processes that are observed in this energy range?

Secondly, new solar neutrino experiments will provide accurate measurements of the fluxes of the important p–p and ^{7}Be solar neutrino fluxes, which together amount to $>98\%$ of the total flux of solar neutrinos predicted by the standard solar model. These measurements will test the solar model predictions for the main energy-producing reactions, predictions that are more precise than for the higher-energy neutrinos. Using only the measurements of the solar neutrino fluxes, one can determine the current rate at which energy is being produced in the solar interior and can compare that energy generation rate with the observed photon luminosity emitted from the solar surface. This comparison will constitute a direct and accurate test of the fundamental idea that the Sun shines by nuclear reactions among light elements. Moreover, the neutrino flux measurements will test directly a general result of the standard solar model, namely, that the Sun is in a quasi-steady state in which the interior energy generation rate equals the surface radiation rate.

Thirdly, future solar neutrino experiments will make possible a precise measurement of the vacuum mixing angle, θ_{12}, as well as a slightly improved constraint on θ_{13}. The increased robustness in determining mixing angles will be very useful in connection with searches for CP violation. Uncertainties in the CP-conserving neutrino parameters probably compromise the determination of the CP violating phase.

Fourthly, there may be entirely new physical phenomena that show up only at the low energies, the very long baseline, and the great sensitivity to matter effects provided by solar neutrino experiments. It may be recalled that solar neutrino research was initiated to study the solar interior, not to search for neutrino oscillations. Recently, two possibilities have been discussed in which new physics that is compatible with all present data could show up at low energies in solar neutrino experiments. (1) There could be a sterile neutrino with very small mixing to active neutrinos and with a mass splitting smaller than the solar LMA splitting [52]. If so, matter effects in the Sun would resonantly enhance the mixing, producing at energies

around 1 MeV a much stronger deficit than expected from pure LMA oscillations. (2) There could be non-dominant flavour-changing neutrino–matter interactions. In that case, the predicted day–night asymmetry in the lower part of the LMA region ($\Delta m^2 \sim 10^{-5}$) can be very small, making the solar allowed region compatible with the lowest 90% CL region allowed by KamLAND (see the right panel of figure 4). These non-standard interactions would profoundly modify the conversion probability at low energies. The probability that a ν_e neutrino would remain a ν_e could be a factor of two smaller than expected by pure LMA oscillations at the pep line (where $P_{ee}^{LMA} \sim 0.6$), if non-standard interactions are around 10% of the standard coupling (G_F) ([53]). A measurement of the neutrino flux in the pep line will be sensitive to these non-standard interactions, which are unobservable at higher energies. The discovery of either mechanism, sterile neutrinos or flavour-changing neutrino interactions, would have strong particle physics implications.

In this paper, we have assumed the correctness of all solar neutrino and reactor experiments that have been performed so far or which will be performed in the future. But the history of science teaches us that this is a dangerous assumption. Sometimes, unrecognized systematic uncertainties can give misleading results. To be sure that our conclusions are robust, the same quantities must be measured in different ways.

6.2. A ^{7}Be experiment

The existing solar plus reactor experiments provide only loose constraints on the ^{7}Be solar neutrino flux, corresponding to approximately a $\pm 40\%$ uncertainty at 1σ. We need an experiment to measure directly the flux of ^{7}Be solar neutrinos!

How accurate should be the ^{7}Be experiment to provide important new information? A measurement of the ν–e scattering rate accurate to $\pm 10\%$ or better will reduce by a factor of four the uncertainty in the measured ^{7}Be neutrino flux. Moreover, the 10% ^{7}Be flux measurement will reduce the uncertainty in the crucial p–p flux by a factor of about 2.5. That improved determination of the p–p flux by a ^{7}Be measurement is due to the luminosity constraint. A ^{7}Be measurement accurate to $\pm 3\%$ would provide another factor of two improvement in the accuracy of the ^{7}Be and p–p solar neutrino fluxes.

All of these improvements are measured with respect to what we expect can be achieved with three years of operation of the KamLAND experiment. Comparable information can be obtained from a charged-current (neutrino absorption) experiment and from a neutrino–electron scattering experiment if both are performed to the same accuracy.

Contrary to what some authors have stated, a ^{7}Be solar neutrino experiment is not expected to provide significantly more accurate values for the neutrino oscillation parameters than what we think will be available after three years of operation of KamLAND.

6.3. A p–p experiment

According to the standard solar model, about 91% of the total flux of the neutrinos from the Sun is in the form of the low energy (<0.42 MeV) p–p neutrinos. We cannot be sure that we have a correct description of the solar interior until this fundamental prediction is tested. Moreover, the p–p neutrinos are in the range where vacuum oscillations dominate over matter effects, hence observing these low-energy neutrinos is also an opportunity to test in a crucial way our understanding of the neutrino physics.

Figure 2 shows that, for the currently LMA favoured oscillation scenario, the survival probability, P_{ee}, increases by about a factor of two in going from high neutrino energies (at which ^{8}B neutrinos are detected) to low energies (at which p–p neutrinos can be observed). This transition from matter-dominated oscillations to vacuum-dominated oscillations is a fundamental prediction of the favoured LMA oscillation solution. Since we already know the p–p flux to an accuracy of $\pm 2\%$ from existing experiments (see equation (13)), we can use the measured rate of a p–p experiment (or a pep experiment) to test whether the predicted transition from matter-dominated to vacuum-dominated oscillations actually occurs. This test will become even more powerful after a ^{7}Be experiment is performed since the ^{7}Be measurement will, together with the luminosity constraint, make our experimental determination of the p–p neutrino flux even more precise (see the discussion in section 6.2).

If we really know what we think we know, if the standard solar model is correct to the stated accuracy ($\pm 1\%$ for the total p–p neutrino flux) and if there is no new physics that shows up below 0.4 MeV, then a measurement of the p–p flux to an accuracy of better than $\pm 3\%$ is necessary to improve significantly our experimental knowledge of $\tan^2\theta_{12}$. The main reason why such a high accuracy is required is that the existing experiments, if they are all correct to their quoted accuracy, already determine the p–p solar neutrino flux to $\pm 2\%$. (We assume that three years of KamLAND reactor data will be available, as well as a $\pm 5\%$ measurement of the ^{7}Be neutrino–electron scattering rate.)

As described above, an accurate measurement of the p–p solar neutrino flux will provide a direct test of the fundamental ideas underlying the standard solar model. The p–p measurement will make possible the determination of the total solar luminosity from just neutrino experiments alone. The neutrino luminosity can be compared with the photon luminosity to check whether nuclear fusion reactions among light elements is the only discernible source of solar energy and whether the Sun is in an approximate steady state in which the rate of interior energy generation equals the rate at which energy is radiated through the solar surface. The global combination of a ^{7}Be experiment, plus a p–p experiment, plus the existing solar data, and three years of KamLAND would make possible a precise determination of the solar neutrino luminosity. A p–p solar neutrino experiment accurate to 5% would make possible a measurement of the solar neutrino luminosity to 4% and a 1% p–p experiment would determine the solar luminosity to the accuracy implied below:

$$\frac{L_\odot \text{ (neutrino-inferred)}}{L_\odot} = 0.99 \pm 0.02. \tag{24}$$

6.4. A pep experiment

Assuming that the pep neutrino flux (a 1.4 MeV neutrino line) is measured instead of the p–p neutrino flux, we repeated the global analyses of existing and future solar and KamLAND data. The global analyses show that a measurement of the ν–e scattering rate by pep solar neutrinos would, assuming only standard interactions, yield essentially equivalent information about neutrino oscillation parameters and solar neutrino fluxes as a measurement of the ν–e scattering rate by p–p solar neutrinos. The estimated best-estimates and uncertainties in the parameters are almost identical for the analyses we have carried out for p–p and pep neutrinos.

A measurement of pep neutrinos would require a more massive detector than is required to study pp neutrinos, since the pep flux is more than two orders of magnitude smaller than the pp flux. On the other hand, pep neutrinos are more sensitive than pp neutrinos to non-standard matter effects (see discussion in section 6.1).

6.5. Proton decay experiments and solar neutrino measurements

Large water Cherenkov detectors can provide a unique and important test of matter oscillations using ^{8}B solar neutrinos. Only a very large detector will have an event rate that is sufficiently high to detect with statistical confidence the day–night effect with solar neutrinos, an effect which is a characteristic signal of matter-induced neutrino oscillations (the MSW effect).

Motivated by the UNO proposal [54], we suppose for specificity that a future Cherenkov detector will have a fiducial volume seven times that of Super-Kamiokande and that this detector can measure neutrino–electron scattering above 6 MeV. We also assume that the backgrounds and the photo-multiplier coverage ($\sim$40%) will be similar to the Super-Kamiokande experiment.

The best-fit LMA solution predicts a 2% day–night difference in ν–e scattering event rates, which can be observed as a 4σ effect in approximately 10 years. A water Cherenkov proton decay experiment would also provide a much more precise measurement (much better than 1%) of the total event rate for the scattering of ^{8}B solar neutrinos by electrons.

A first detection of the very rare but high energy hep neutrinos should also be possible. We estimate that a measurement of the hep flux with the hypothesized proton decay detector should achieve a 4σ or better accuracy over 10 years. This result assumes that the BP04 predicted hep flux is correct.

For these measurements of solar neutrinos to be successful, the proton decay detector should be placed at a good depth with an active shield. Special care should be taken to make sure that radon contamination is low. Frequent calibrations should be made to ensure that the detector sensitivity and the detector threshold do not vary significantly, in an unknown way, from day to night. The procedure for performing the day–night calibrations should be included in the planning for the next generation proton decay detector.

The study of solar neutrinos using large water Cherenkov detectors is an ideal complement to the study of nucleon decay. The event rate for nucleon decay cannot be predicted with confidence, although the importance of just one or a few events is enormous. The event rate for ^{8}B solar neutrinos can be predicted with great confidence and is enormous, about 31 100 events per year.

Somewhat paradoxically, the study of ^{8}B solar neutrinos could turn out to be the bread and butter project of next generation water Cherenkov proton decay detectors.

Acknowledgments

JNB and CPG acknowledge support from NSF grant no. PHY0070928.

References

[1] Gribov V N and Pontecorvo B M 1969 *Phys. Lett.* B **28** 493
[2] Wolfenstein L 1978 *Phys. Rev.* D **17** 2369
Mikheyev S P and Smirnov A Y 1985 *Sov. J. Nucl. Phys.* **42** 913

[3] Bahcall J N 1989 *Neutrino Astrophysics* (Cambridge: Cambridge University Press)
[4] Bahcall J N, Pinsonneault M H and Basu S 2001 *Astrophys. J.* **555** 990
[5] Cabibbo N 2002 *Int. J. Mod. Phys.* A **17** 3500
[6] Fiorentini G and Ricci B 2002 *Phys. Lett.* B **526** 186
[7] Gonzalez-Garcia M C and Nir Y 2003 *Rev. Mod. Phys.* **75** 345
[8] Smirnov A Yu 2003 *Proc. X Int. Workshop on Neutrino Telescopes, Venice*, *11–14 March* ed M B Ceolin
[9] Bahcall J N and Peña-Garay C 2003 *J. High Energy Phys.* **11** 004
[10] Barger V, Marfatia D and Whisnat K 2003 *Int. J. Mod. Phys.* E **12** 569
[11] Bilenky S M, Giunti C, Grifols J A and Masso E 2003 *Phys. Rep.* **379** 69
[12] Kayser B 2003 *Nucl. Phys. Proc.* **118** (Suppl.) 425
[13] Murayama H 2002 *Int. J. Mod. Phys.* A **17** 3403
[14] Fogli G L, Lisi E, Marrone A and Palazzo A 2004 *Phys. Lett.* B **583** 149
[15] Maltoni M, Schwetz T, Tortola M A and Valle J W F 2003 *Phys. Rev.* D **68** 113010
[16] Choubey S, Goswami S, Kar K, Antia H M and Chitre S M 2001 *Phys. Rev.* D **64** 113001
[17] Boothroyd A I and Sackmann I-J 2003 *Astrophys. J.* **583** 1004
[18] Couvidat S, Turck-Chieze S and Kosovichev A G 2003 *Astrophys. J.* **599** 1434
[19] Haxton W C and Holstein B R 2004 *Am. J. Phys.* **72** 18
[20] McDonald A 2004 *New J. Phys.* submitted
[21] Bahcall J N, Pinsonneault M H, Basu S and Christensen-Dalsgaard J 1997 *Phys. Rev. Lett.* **78** 171
[22] Bahcall J N and Pinsonneault M H 2004 *Phys. Rev. Lett.* **92** 121301
[23] Bahcall J N 1997 *Phys. Rev.* C **56** 3391
Bahcall J N, Lisi E, Alburger D E, De Braeckeleer L, Freedman S J and Napolitano J 1996 *Phys. Rev.* C **54** 411
[24] Allende Prieto C, Lambert D L and Asplund M 2002 *Astrophys. J.* **573** L137
Allende Prieto C, Lambert D L and Asplund 2001 *Astrophys. J.* **556** L63
Asplund M, Grevesse N and Sauval A J 2004 *Astron. Astrophys.* in press; see also *Preprint* astro-ph/0312290
Asplund M 2004, private communication
Asplund M, Nordlund A, Trampedach R and Stein R F 2000 *Astron. Astrophys.* **359** 743
Asplund M 2000 *Astron. Astrophys.* **359** 755
[25] Junghans A R *et al* 2003 *Phys. Rev.* C **68** 065803
Baby L T *et al* (ISOLDE Collaboration) 2003 *Phys. Rev. Lett.* **90** 022501
Baby L T *et al* (ISOLDE Collaboration) 2003 *Phys. Rev.* C **67** 065805
Hammache F *et al* 1998 *Phys. Rev. Lett.* **80** 928
Hammache F *et al* 2001 *Phys. Rev. Lett.* **86** 3985
Hass M, Broude C, Fedoseev V, Goldring G, Huber G, Lettry J, Mishin V, Ravn H J, Sebastian V and Weissman L (ISOLDE Collaboration) 1999 *Phys. Lett.* B **462** 237
Strieder F *et al* 2001 *Nucl. Phys.* A **696** 219
Junghans A R, Mohrmann E C, Snover K A, Steiger T D, Adelberger E G, Casandjian J M, Swanson H E, Buchmann L, Park S H and Zyuzin A 2002 *Phys. Rev. Lett.* **88** 041101
[26] Park T S, Marcucci L E, Schiavilla R, Viviani M, Kievsky A, Rosati S, Kubodera K, Min D-P and Rho M 2003 *Phys. Rev.* C **67** 055206
[27] Rogers F J and Nayfonov A 2002 *Astrophys. J.* **576** 1064
Rogers F J 2001 *Contrib. Plasma Phys.* **41** 179
[28] Grevesse N and Sauval A J 1998 *Space Sci. Rev.* **85** 161
[29] Adelberger E G *et al* 1998 *Rev. Mod. Phys.* **70** 1265
[30] Angulo C and Descouvemont P 2001 *Nucl. Phys.* A **690** 755
LUNA Collaboration 2003 *Phys. Lett.* B nucl-ex/0312015 submitted
[31] Bahcall J N, Gonzalez-Garcia M C and Peña-Garay C 2003 *J. High Energy Phys.* **2** 009
[32] Bahcall J N, Fowler W A, Iben I and Sears R L 1963 *Astrophys. J.* **137** 344
Bahcall J N 2003 *Nucl. Phys.* B (Proc. Suppl.) **118** 77

[33] Eguchi K *et al* 2003 *Phys. Rev. Lett.* **90** 021802
[34] Gluza J and Zralek M 2001 *Phys. Lett.* B **517** 158
[35] Kuo T K and Pantaleone J 1986 *Phys. Rev. Lett.* **57** 1805
[36] Shi X and Schramm D N 1992 *Phys. Lett.* B **283** 305
[37] Apollonio M *et al* 1999 *Phys. Lett.* B **466** 415
[38] Boehm F *et al* 2000 *Phys. Rev.* D **62** 072002
[39] Gonzalez-Garcia M C and Peña-Garay C 2003 *Phys. Rev.* D **68** 093003
[40] Bethe H A 1986 *Phys. Rev. Lett.* **56** 1305
[41] Mikheev S P and Smirnov A Y 1986 *Proc. 6th Moriond Workshop on Massive Neutrinos in Astrophysics and Particle Physics* ed O Fackler and J Tran Thanh Van (Gif-sur-Yvette: Editions Frontieres) p 355
[42] Messiah A 1986 *Proc. 6th Moriond Workshop on Massive Neutrinos in Astrophysics and Particle Physics* ed O Fackler and J Tran Thanh Van (Gif-sur-Yvette: Editions Frontieres) p 373
[43] Bahcall J N 2002 *Phys. Rev.* C **65** 025801
[44] Bahcall J N, Gonzalez-Garcia M C and Peña-Garay C 2003 *Phys. Rev. Lett.* **90** 131301
[45] Murayama H and Peña-Garay C 2003 *Phys. Rev.* D **69** 031301
[46] Coleman S R and Glashow S L 1997 *Phys. Lett.* B **405** 249
[47] Coleman S R and Glashow S L 1999 *Phys. Rev.* D **59** 116008
[48] Colladay D and Kostelecky V A 1997 *Phys. Rev.* D **55** 6760
[49] Barger V D, Pakvasa S, Weiler T J and Whisnant K 2000 *Phys. Rev. Lett.* **85** 50555
[50] Bahcall J N, Barger V D and Marfatia D 2002 *Phys. Lett.* B **534** 120
[51] Murayama H 2003 *Preprint* hep-ph/0307127
[52] de Holanda P C and Smirnov A Y 2003 *Preprint* hep-ph/0307266
Berezinsky V, Narayan M and Vissani F 2003 *Nucl. Phys.* B **658** 254
[53] Friedland A, Lunardini C and Peña-Garay C 2004 *Preprint* hep-ph/0402266
[54] UNO Proto-collaboration 2000 UNO Whitepaper: Physics Potential and Feasibility of UNO, SBHEP-01-03(2000), http://nngroup.physics.sunysb.edu/uno/
Jung C K 2002 *Preprint* hep-ex/0005046